arXiv:1702.01710v1 [cond-mat.stat-mech] 6 Feb 2017

The thermal density matrix of a charged particle in an external magnetic field in twisted periodic boundary conditions

Tamás Haidekker Galambos and Csaba Tőke
BME-MTA Exotic Quantum Phases "Lendület" Research Group, Budapest University of Technology and Economics, Institute of Physics, Budafoki út 8, H-1111 Budapest, Hungary

(Dated: February 7, 2017)

We provide closed-form expressions for the thermal density matrix (or the Euclidean propagator) of a charged particle in a uniform external magnetic field on the flat torus under very general conditions. We propose this formula for use in phase-fixed path integral Monte Carlo simulation of time-reversal symmetry breaking systems, including quantum Hall systems and rotating Bose-Einstein condensates.

PACS numbers: 05.30.-d,02.70.Ss

I. INTRODUCTION

The thermal density matrix (which is closely related to the Euclidean or imaginary-time propagator) $\rho(\mathbf{r},\mathbf{r}';\beta) = \langle\mathbf{r}'|e^{-\beta\mathcal{H}}|\mathbf{r}\rangle$ of a single particle encodes basic information on the thermodynamics in noninteracting systems, and it serves as a natural starting point in diagrammatic methods or in the numerical modeling of interacting systems by the path-integral Monte Carlo [1] and the path-integral ground state [2] methods, which yield information on the equilibrium properties of interacting many-body systems at finite and zero temperature, respectively. For numerical simulations of interacting systems by the Monte Carlo method we unavoidably have to work with finite, and often quite small, systems. Our starting point is therefore the density matrix in some compact geometry, using periodic or twisted [3, 4] boundary conditions in cubic domain or on the sphere [5]. In this paper we discuss a case that is apparently neglected in the literature, namely the thermal density matrix on the flat torus in the presence of an external magnetic field, which we will assume to be perpendicular to the surface. (The addition of a third dimension that is parallel to the external field is trivial.) We will provide closed-form analytic expressions for the density matrix, assuming only a mild geometric constraint, and allowing for twisted boundary conditions.

The motion of a charged particle in an external homogeneous magnetic field is known to be related to one-dimensional harmonic motion; assuming the particle moves in the xy plane with open boundary conditions, a simple calculation in the Landau gauge $\mathbf{A} = -By\hat{\mathbf{x}}$ yields

$$\rho^{\mathrm{open}}(\mathbf{r},\mathbf{r}';\beta) = \sum_{n=0}^{\infty}\int dk\; \eta^*_{nk}(\mathbf{r}')\eta_{nk}(\mathbf{r})e^{-\beta\hbar\omega_c(n+1/2)} = \\ = \frac{1}{2\pi\ell^2}\frac{\sqrt{u}}{1-u}e^{-\frac{1}{4\ell^2}\frac{1+u}{1-u}|\mathbf{r}-\mathbf{r}'|^2+\frac{i(x'-x)(y+y')}{2\ell^2}}, \quad (1)$$

where $\omega_c = \frac{eB}{m}$ is the cyclotron frequency, $\ell = \sqrt{\frac{\hbar}{eB}}$ is the magnetic length, $\beta = \frac{1}{k_B T}$ is the inverse temperature, $u = e^{-\beta\hbar\omega_c}$, and η_{nk}'s are the Landau orbitals on the infinite plane:

$$\eta_{nk}(x,y) = \frac{e^{ikx}}{\sqrt{2\pi}}\frac{1}{\sqrt{\sqrt{\pi}\ell 2^n n!}}H_n\left(y_k\right)e^{-\frac{1}{2}y_k^2}, \quad (2)$$
$$y_k = \frac{y}{\ell} - k\ell.$$

Just like its time-reversal symmetric counterpart, $\rho(\mathbf{r},\mathbf{r}';\beta)$ describes diffusive motion in imaginary time (inverse temperature), but it also has a gauge-dependent phase factor. Compared to the case without the external magnetic field, the diffusion process described by Eq. (1) is slower; for large imaginary time β the width of the Gaussian $|\rho^{\mathrm{open}}(\mathbf{r},\mathbf{r}';\beta)|$ tends to a finite value determined by the magnetic length. In the other limit, $\beta\hbar\omega_c \ll 1$ this Gaussian grows with the same rate as in the absence of the magnetic field.

We will show below that in the small imaginary time limit the above properties survive qualitatively on the torus, i.e., if $\mathbf{r}'$ is fixed, the propagator describes a growing Gaussian around $\mathbf{r}'$ and its periodic images with an appropriate phase factor. For larger β, however, these Gaussians start to overlap, giving rise to a complex interference pattern with a slowly evolving pattern of zeros in the principal domain (the paralelogram whose opposite sides are connected by twisted boundary conditions). These zeros prevent the noninteracting particles from accessing parts of the torus; this may raise issues in path-integral Monte Carlo simulations.

The paper is structured as follows. In Sec. II we review the properties of the single-particle orbitals on the torus. In Sec. III we derive the thermal density matrix, and analyze its basic properties, and discuss the means of its efficient computation. In Sec. IV we conclude with an outlook on possible applications.

II. SINGLE-PARTICLE STATES ON THE TORUS

In the gauge $\mathbf{A} = -By\hat{\mathbf{x}}$ that is used throughout this article, the states in the *lowest* Landau level assume the

form [4]

$$\psi_0(z) = f(z)e^{-\frac{y^2}{2\ell^2}}, \tag{3}$$

where $z = x+iy$ is the complex coordinate of the particle on the plane, and $f(z)$ is a holomorphic function. The appropriate translations in the presence of a perpendicular magnetic field are the magnetic translations [6]:

$$t(\mathbf{L}) = \exp\left(\frac{i}{\hbar}\mathbf{L}\cdot\mathbf{p} - i\frac{\hat{\mathbf{z}}\cdot(\mathbf{L}\times\mathbf{r})}{\ell^2}\right), \tag{4}$$

where $\mathbf{p} = \frac{\hbar}{i}\nabla - e\mathbf{A}$ is the canonical momentum. In the current gauge, magnetic translations act as $t(\mathbf{L})\psi(\mathbf{r}) = \exp(\frac{ix\hat{\mathbf{y}}\cdot\mathbf{L}}{\ell^2})\psi(\mathbf{r}+\mathbf{L})$. Consider a parallelogram spanned by two nonparallel vectors $\mathbf{L}_1 = (L_1, 0)$ and $\mathbf{L}_2 = (L_2\cos\theta, L_2\sin\theta)$. A torus is obtained by identifying the the opposite sides of this unit cell, c.f. Fig. 1(a). We will

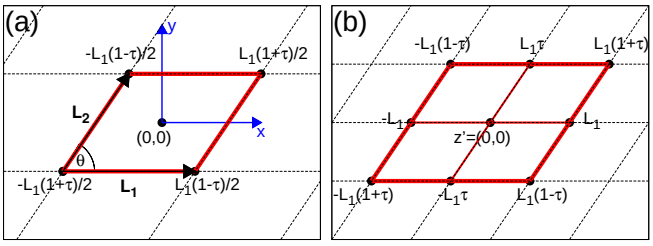

FIG. 1: (a) The principal domain of the torus with definitions used in the text. (b) The quadruple domain used for finding the zeros of the density matrix in the low-temperature limit.

require that the orbitals obey twisted boundary conditions with twist angles $\phi_{1,2}$,

$$t(\mathbf{L}_{1,2})\psi(\mathbf{r}) = e^{i\phi_{1,2}}\psi(\mathbf{r}). \tag{5}$$

These conditions are mutually compatible only if the parallelogram is pierced by an integral number of flux quanta,

$$N_\phi = \frac{|\mathbf{L}_1\times\mathbf{L}_2|}{2\pi\ell^2} = \frac{L_1L_2\sin\theta}{2\pi\ell^2}. \tag{6}$$

Then the parallelogram spanned by $\mathbf{L}_1$ and $\mathbf{L}_2$ qualifies as a magnetic unit cell.

We seek the holomorphic part $f(z)$ of the lowest Landau level eigenstates in terms of Jacobi elliptic functions with characteristics [7]

$$\vartheta\begin{bmatrix}a\\b\end{bmatrix}(z|\tau) = \sum_n e^{i\pi\tau(n+a)^2+2i(n+a)(z+b\pi)}. \tag{7}$$

(Traditionally defined Jacobi elliptic functions correspond to $\vartheta\begin{bmatrix}\frac{1}{2}\\\frac{1}{2}\end{bmatrix}(z|\tau) = -\vartheta_1(z|\tau)$, $\vartheta\begin{bmatrix}\frac{1}{2}\\0\end{bmatrix}(z|\tau) = \vartheta_2(z|\tau)$, $\vartheta\begin{bmatrix}0\\0\end{bmatrix}(z|\tau) = \vartheta_3(z|\tau)$, and $\vartheta\begin{bmatrix}0\\\frac{1}{2}\end{bmatrix}(z|\tau) = \vartheta_4(z|\tau)$. Notice that sometimes a factor π is factored out of the argument, i.e., $\vartheta\begin{bmatrix}a\\b\end{bmatrix}(\frac{z}{\pi}|\tau)$ is defined.) The boundary conditions in Eq. (5) yield N_ϕ distinct states [8, 9],

$$\psi_{0m}(z) = \frac{1}{\sqrt{\ell L_1\sqrt{\pi}}}\vartheta\begin{bmatrix}a_m\\b_m\end{bmatrix}\left(\frac{\pi N_\phi z}{L_1}\middle|N_\phi\tau\right)e^{-\frac{y^2}{2\ell^2}}, \tag{8}$$

$m = 0, 1, \ldots, (N_\phi-1)$, with $\tau = \frac{L_2}{L_1}e^{i\theta}$, and

$$a_m = \frac{\phi_1}{2\pi N_\phi} + \frac{m}{N_\phi}, \quad b_m = -\frac{\phi_2}{2\pi} - \frac{N_\phi\Re\tau}{2}. \tag{9}$$

Notice that $\psi_{0m}(z)$, together with its higher Landau level descendants that follow later, is normalized for a magnetic unit cell,

$$\int_0^{L_2\sin\theta}dy\int_{y\cot\theta}^{y\cot\theta+L_1}dx\psi^*_{n'm'}(x+iy)\psi_{nm}(x+iy) = \\ = \delta_{nn'}\delta_{mm'}. \tag{10}$$

We note that this particular basis corresponds to a string arrangement [4] of zeros of the holomorphic function $f(z)$ in the magnetic unit cell.

The orbitals in higher Landau levels are obtained by the application of Landau level ladder operators,

$$\psi_{nm}(z) = \frac{(a^\dagger)^n}{\sqrt{n!}}\psi_{0m}(z), \tag{11}$$

where

$$\hat{a}^\dagger = i\ell\sqrt{2}\left(\partial_z - iA_z\right), \tag{12}$$

with $\partial_z = \frac{1}{2}(\partial_x - i\partial_y)$ and $A_z = \frac{1}{2}(A_x - iA_y)$. In our particular gauge,

$$\hat{a}^\dagger = \frac{\ell}{\sqrt{2}}\left(i\partial_x + \partial_y - \frac{y}{\ell^2}\right). \tag{13}$$

The degeneracy of each Landau level is N_ϕ. Straightforward algebra yields

$$\psi_{nm}(z) = \frac{(-1)^n}{\sqrt{2^n n!\ell L_1\sqrt{\pi}}}\sum_{p=-\infty}^{\infty}H_n\left(\frac{y+C_{p,m}}{\ell}\right) \\ \times\exp\left(i\pi\tau N_\phi(p+a_m)^2 + 2\pi i(p+a_m)b_m\right) \\ \times\exp\left(\frac{C_{p,m}^2}{2\ell^2} + \frac{iC_{p,m}x}{\ell^2} - \frac{(y+C_{p,m})^2}{2\ell^2}\right), \tag{14}$$

where $C_{p,m} = \frac{2\pi N_\phi\ell^2}{L_1}(p+a_m) = L_1(p+a_m)\Im\tau$.

III. THE THERMAL DENSITY MATRIX

Using the orbitals of Eq. (14) in the definition of the density matrix,

$$\rho(\mathbf{r},\mathbf{r}';\beta) = \sum_{n=0}^{\infty}\sum_{m=0}^{N_\phi-1}\psi_{nm}(\mathbf{r})\psi^*_{nm}(\mathbf{r}')u^{n+\frac{1}{2}}. \tag{15}$$

and performing the n-summation by Mehler's formula, we obtain

$$\rho(\mathbf{r},\mathbf{r}';\beta)=\frac{\sqrt{u}}{\ell L_1\sqrt{\pi}\sqrt{1-u^2}}\sum_{m=0}^{N_\phi-1}\sum_{p,p'=-\infty}^{\infty}\exp\big(i\pi\tau N_\phi(p+a_m)^2-i\pi\tau^* N_\phi(p'+a_m)^2+2\pi i(p+a_m)b_m-$$
$$-2\pi i(p'+a_m)b_m+\frac{C_{p,m}^2}{2\ell^2}+\frac{iC_{p,m}x}{\ell^2}+\frac{C_{p',m}^2}{2\ell^2}-\frac{iC_{p,m}x'}{\ell^2}\Big)\exp\left(-\frac{1}{2}\frac{1+u^2}{1-u^2}(A^2+B^2)+\frac{2uAB}{1-u^2}\right),\quad(16)$$

with $A=\frac{y+C_{p,m}}{\ell}$ and $B=\frac{y'+C_{p',m}}{\ell}$.

Introducing new summation variables $n_1=p+p'$ and $n_2=p-p'$, double-counting is avoided if n_1,n_2 are either both even or both odd. This decouples the summation variables in all terms except for a factor of $\exp(i\pi N_\phi n_1 n_2\Re\tau)$. This can be omitted if $N_\phi\Re\tau=k$ is an integer, i.e.,

$$L_2\cos\theta=\frac{kL_1}{N_\phi}.\quad(17)$$

Notice that L_1/N_ϕ is the separation of the guiding centers of orbitals in the $\mathbf{L}_1$ direction; Eq. (17) simply states that a translation by $\mathbf{L}_2$ should be compatible with these guiding center positions. The rectangular torus, most relevant for simulations, trivially fulfills Eq. (17). Then by simple algebra and by the definition in Eq. (7) we obtain

$$\rho(\mathbf{r},\mathbf{r}';\beta)=\frac{\sqrt{u}}{\ell L_1\sqrt{\pi}\sqrt{1-u^2}}\times\exp\left(-\frac{1}{2\ell^2}\frac{1+u^2}{1-u^2}(y^2+y'^2)+\frac{2u}{1-u^2}\frac{yy'}{\ell^2}\right)$$
$$\times\sum_{m=0}^{N_\phi-1}\left\{\vartheta\begin{bmatrix}a_m\\0\end{bmatrix}(z_1|\tau_1)\vartheta\begin{bmatrix}0\\2b'_m\end{bmatrix}(z_2|\tau_2)+\right.$$
$$\left.+(-1)^k\vartheta\begin{bmatrix}a_m+\frac{1}{2}\\0\end{bmatrix}(z_1|\tau_1)\vartheta\begin{bmatrix}\frac{1}{2}\\2b'_m\end{bmatrix}(z_2|\tau_2)\right\},\quad(18)$$

where $b'_m=b_m+N_\phi a_m\Re\tau$, and

$$\tau_1=i\pi\left(\frac{2\ell N_\phi}{L_1}\right)^2\frac{1-u}{1+u},\quad(19)$$
$$z_1=\frac{N_\phi\pi}{L_1}\left(x-x'+i(y+y')\frac{1-u}{1+u}\right),\quad(20)$$
$$\tau_2=i\pi\left(\frac{2\ell N_\phi}{L_1}\right)^2\frac{1+u}{1-u},\quad(21)$$
$$z_2=\frac{N_\phi\pi}{L_1}\left(x+x'+i(y-y')\frac{1+u}{1-u}\right).\quad(22)$$

The thermal density matrix $\rho(\mathbf{r},\mathbf{r}';\beta)$ obeys the boundary conditions

$$t_{\mathbf{r}}(n\mathbf{L}_1+m\mathbf{L}_2)\rho(\mathbf{r},\mathbf{r}';\beta)=e^{i(n\phi_1+m\phi_2)}\rho(\mathbf{r},\mathbf{r}';\beta),\quad(23)$$
$$t^*_{\mathbf{r}'}(n\mathbf{L}_1+m\mathbf{L}_2)\rho(\mathbf{r},\mathbf{r}';\beta)=e^{-i(n\phi_1+m\phi_2)}\rho(\mathbf{r},\mathbf{r}';\beta),\quad(24)$$

as can be checked by simple algebra.

The density matrix in Eq. (18) can be cast in a more transparent form by the application of a modular transformation $\tau_1\to-\frac{1}{\tau_1}$, $z_1\to\frac{z_1}{\tau_1}$ in the corresponding theta factors:

$$\rho(\mathbf{r},\mathbf{r}';\beta)=\frac{1}{N_\phi}\rho^{\rm open}(\mathbf{r},\mathbf{r}';\beta)$$
$$\times\sum_{m=0}^{N_\phi-1}\left\{\vartheta\begin{bmatrix}0\\a_m\end{bmatrix}\left(\frac{z_1}{\tau_1}\Big|\tau'_1\right)\vartheta\begin{bmatrix}0\\2b'_m\end{bmatrix}(z_2|\tau_2)+\right.$$
$$\left.+(-1)^k\vartheta\begin{bmatrix}0\\a_m+\frac{1}{2}\end{bmatrix}\left(\frac{z_1}{\tau_1}\Big|\tau'_1\right)\vartheta\begin{bmatrix}\frac{1}{2}\\2b'_m\end{bmatrix}(z_2|\tau_2)\right\},\quad(25)$$

where $\tau'_1=\left(\frac{L_1}{2\ell N_\phi\sqrt{\pi}}\right)^4\tau_2$, and $\frac{z_1}{\tau_1}=\frac{L_1}{4\ell^2N_\phi}\left(y+y'+i(x'-x)\frac{1+u}{1-u}\right)$. We could factor out the density matrix for open boundary conditions in Eq. (25) because both the gauge-dependent phase, the Gaussian factor of the coordinate differences, and the temperature dependent prefactor were identical. The sum of pair products of theta functions ensures the proper periodicity according to Eqs. (23-24). The two equivalent expressions in Eqs. (18) and Eq. (25) are the main results of this paper. The latter has a more transparent structure, as the x- and y-components of the difference vector $\mathbf{r}-\mathbf{r}'$ and the center-of-mass vector $\frac{\mathbf{r}+\mathbf{r}'}{2}$ appear on the same footing in the theta functions.

We note that $|\rho(\mathbf{r},\mathbf{r}';\beta)|$ is *not* invariant for a simultaneous displacement of both $\mathbf{r}$ and $\mathbf{r}'$ by the same vector $\mathbf{d}$, which corresponds to choosing a shifted magnetic unit cell on the plane for compactification by periodic boundary conditions, except for special choices of $\mathbf{d}$. This is understood easily by noting that the second characteristic b_m appears in Eq. (7) as a simple additive constant to the variable z, letting us rewrite Eq. (25) as

$$\rho(\mathbf{r},\mathbf{r}';\beta) = \frac{1}{N_\phi}\rho^{\rm open}(\mathbf{r},\mathbf{r}';\beta)$$
$$\times \sum_{m=0}^{N_\phi-1}\left\{\vartheta\begin{bmatrix}0\\ a_m+\frac{L_1}{4\pi\ell^2 N_\phi}(y+y')\end{bmatrix}\left(\frac{\pi N_\phi\tau_1'}{L_1}(x'-x)\Big|\tau_1'\right)\vartheta\begin{bmatrix}0\\ 2b_m'+\frac{N_\phi}{L_1}(x+x')\end{bmatrix}\left(\frac{\pi(y-y')\tau_2}{2L_2\sin\theta}\Big|\tau_2\right)+\right.$$
$$\left.+(-1)^k\vartheta\begin{bmatrix}0\\ a_m+\frac{1}{2}+\frac{L_1}{4\pi\ell^2 N_\phi}(y+y')\end{bmatrix}\left(\frac{\pi N_\phi\tau_1'}{L_1}(x'-x)\Big|\tau_1'\right)\vartheta\begin{bmatrix}\frac{1}{2}\\ 2b_m'+\frac{N_\phi}{L_1}(x+x')\end{bmatrix}\left(\frac{\pi(y-y')\tau_2}{2L_2\sin\theta}\Big|\tau_2\right)\right\}. \quad (26)$$

Then it is clear that the arguments of the theta functions depend on the coordinate differences only, and the center of mass can be incorporated in the characteristics as

$$b_m \to b_m + \frac{N_\phi}{L_1}d_x, \quad a_m \to a_m + \frac{L_1}{2\pi\ell^2 N_\phi}d_y. \quad (27)$$

These in turn correspond to fluxes [10, 11], and the shift of the center of mass corresponds to a change in the twist angles by Eq. (9):

$$\phi_2 \to \phi_2 - \frac{2\pi N_\phi}{L_1}d_x, \quad \phi_1 \to \phi_1 + \frac{L_1}{\ell^2}d_y. \quad (28)$$

Thus the twisted boundary conditions in Eq. (5), and, consequently, $|\rho(\mathbf{r},\mathbf{r}';\beta)|$, are invariant only if

$$\mathbf{d} = \left(\frac{L_1}{N_\phi}n_1, \frac{2\pi\ell^2}{L_1}n_2\right) \quad (29)$$

for integral n_1 and n_2.

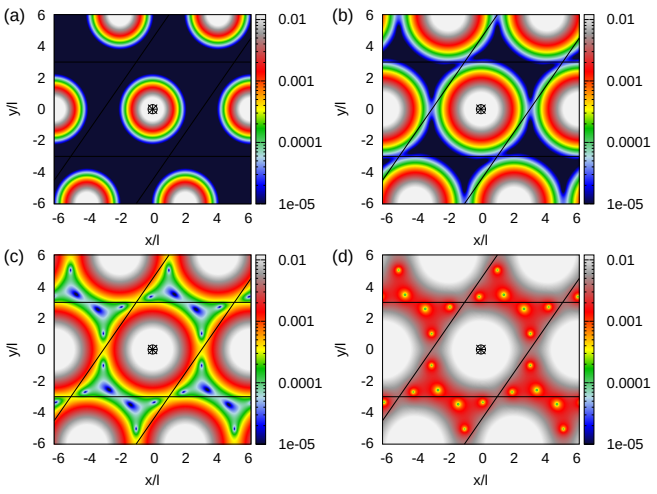

FIG. 2: The dependence of $|\rho(\mathbf{r},\mathbf{r}';\beta)|$ on imaginary time β. There are $N_\phi = 6$ flux quanta in the principal domain, $L_2/L_1 = 1.17$, $\theta \approx 55^\circ$, $\phi_1 = \phi_2 = 0$, and we have fixed $\mathbf{r}'$ at the origin. The panels correspond to $\beta\hbar\omega_c = 0.3$, 0.7, 1.1, and 5, respectively.

The behavior of the density matrix is shown in Fig. 2 for the most general case, i.e., an oblique unit cell. For small imaginary time (high temperature) $|\rho(\mathbf{r},\mathbf{r}';\beta)|$ has a small Gaussian peak around $\mathbf{r}'$, which is fixed at the origin in the figure. This peak spreads out by diffusion as β is increased, and eventually the Gaussians from neighboring unit cells start to overlap appreciably. However, the density matrix also has a phase in an external magnetic field, which gives rise to an interference pattern in this time range. There is destructive interference at certain points, which effectively arrest the diffusion. (We will analyze the zeros of $\rho(\mathbf{r},\mathbf{r}';\beta)$ in the next section.) Beyond a certain β value the picture is essentially stationary.

A. Asymptotic behavior

In the $\beta \to 0$ limit the density matrix must satisfy $\rho(\mathbf{r},\mathbf{r}';\beta) \to \delta(\mathbf{r}-\mathbf{r}')$, and this holds for the density matrix appropriate for open boundary conditions in Eq. (1). Using Eq. (25) and the identities

$$\theta_{3,2}(z|\tau) = \sqrt{\frac{i}{\tau}}\sum_{n=-\infty}^{\infty}(\pm 1)^n \exp\left(-\frac{i\pi}{\tau}\left(n+\frac{z}{\pi}\right)^2\right)$$

one can check that

$$\rho(\mathbf{r},\mathbf{r}';\beta\to 0) = \sum_{k_1,k_2} e^{ik_1\phi_1+ik_2\phi_2-\frac{ixk_2L_2\sin\theta}{\ell^2}}$$
$$\times\,\delta\left(x-x'-k_1L_1-k_2L_2\cos\theta\right)$$
$$\times\,\delta\left(y-y'-k_2L_2\sin\theta\right), \quad (30)$$

which complies with the discrete magnetic translation symmetries in Eqs. (23-24).

Now, in the low-temperature limit, $\beta \to \infty$ ($u \to 0$), the analytic structure of $\rho(\mathbf{r},\mathbf{r}';\beta)$ simplifies significantly. Notice that both for open and periodic boundary conditions the value of the density matrices goes to zero at any fixed coordinates $\mathbf{r}$ and $\mathbf{r}'$. This is an artifact of the zero-point energy $\frac{\hbar\omega_c}{2}$, and does not appear in averages as they involve normalization by the partition function $Z(\beta) = \sum_{n=0}^{\infty}u^{n+1/2} = \frac{\sqrt{u}}{1-u}$. We study the analytic structure in the low-temperature limit by factoring out the nonzero factor $\rho^{\rm open}(\mathbf{r},\mathbf{r}';\beta)$ for convenience:

$$\lim_{\beta\to\infty}\frac{\rho(\mathbf{r},\mathbf{r}';\beta)}{\rho^{\rm open}(\mathbf{r},\mathbf{r}';\beta)} = f_\infty(z,z'), \quad (31)$$

where

$$f_\infty(z,z') = \frac{1}{N_\phi}\sum_{m=0}^{N_\phi-1}\left\{\vartheta\begin{bmatrix}0\\ a_m\end{bmatrix}\left(\frac{iL_1}{4\ell^2 N_\phi}\left(z'^*-z\right)\Big|\tilde\tau_1'\right)\right.$$
$$\times\vartheta\begin{bmatrix}0\\ 2b_m'\end{bmatrix}\left(\frac{N_\phi\pi}{L_1}\left(z+z'^*\right)|\tilde\tau_2\right)+$$
$$+(-1)^k\vartheta\begin{bmatrix}0\\ a_m+\frac{1}{2}\end{bmatrix}\left(\frac{iL_1}{4\ell^2 N_\phi}\left(z'^*-z\right)\Big|\tilde\tau_1'\right)$$
$$\left.\times\vartheta\begin{bmatrix}\frac{1}{2}\\ 2b_m'\end{bmatrix}\left(\frac{N_\phi\pi}{L_1}\left(z+z'^*\right)|\tilde\tau_2\right)\right\}, \quad (32)$$

where

$$\tilde\tau_1' = \frac{i}{\pi}\left(\frac{L_1}{2\ell N_\phi}\right)^2 \quad \text{and} \quad \tilde\tau_2 = i\pi\left(\frac{2\ell N_\phi}{L_1}\right)^2.$$

$f_\infty(z,z')$ is holomorphic in z, and antiholomorphic in z', on the entire complex plane. Fixing z', the zeros $f_\infty(z,z')$ can be counted by the argument principle of complex calculus. We choose the quadruple domain Q with corners $z'+L_1(\pm1\pm\tau)$, c.f. Fig. 1(b). We get

$$\oint_{\partial Q}\frac{d}{dz}\ln\left(f_\infty(z,z')\right)dz = -8\pi i N_\phi, \quad (33)$$

which, exploiting the periodicities in Eqs. (23) to (24) and the fact that $\rho^{\text{open}}(\mathbf{r},\mathbf{r}';\beta)$ is nonzero, implies that the thermal propagator $\rho(\mathbf{r},\mathbf{r}';\beta\to\infty)$ has N_ϕ zeros in the principal domain (c.f. Fig. 1(a)). At nonzero temperature the analytic structure of $\rho(\mathbf{r},\mathbf{r}';\beta)$ is not simple. Nevertheless, we have found numerically that the number of zeros in the principal domain is the same at any finite β, and the zeros very quickly reach their final location. See Fig. (3) for illustration. If N_ϕ is odd, there are zeros that do not move at all. For $\phi_1=\phi_2=0$, in particular, one of them is located in the corners of the principal domain (which are identical by periodicity). Fig. 4 shows the structure of zeros for different geometries. Multiple zeros occur in regular cases, e.g., the square unit cell, panel(b), and the hexagonal one, panel(d).

The point of introducing twist angles in Eq. (5) is that averaging over ϕ_1 and ϕ_2 helps us reduce finite-size effects of the kinetic energy in quantum Monte Carlo. In Fig. 5 we demonstrate the motion of the zeros of the thermal density matrix as we tune the twist angles. Qualitatively, the motion of the zeros shows an interesting analogy with the Hall current: tuning ϕ_1 moves them in the $\mathbf{L}_2$ direction–the direction of the electromotive force on a charged particle induced by the change of flux–, and conversely.

B. Computational considerations

While our first formula for the thermal density matrix, Eq. (18), and the ones we obtain by modular transformation of either [c.f. Eqs. (25) and (A.1)] or both Jacobi

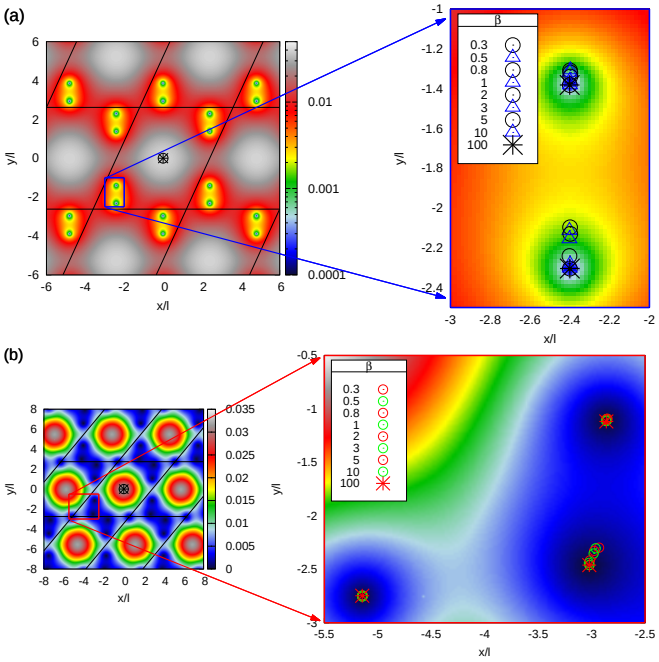

FIG. 3: (a) The low-temperature limit $\beta\to\infty$ of the thermal density matrix for $N_\phi=4$, $\theta\approx65°$, $|\mathbf{L}_2|/|\mathbf{L}_1|=1.2$, $\phi_1=\phi_2=0$. In the zoomed area we show how the zeros move to their asymptotic position as a function of inverse temperature β. (b) The same for $N_\phi=5$, $\theta\approx50°$, $|\mathbf{L}_2|/|\mathbf{L}_1|=1.25$, $\phi_1=\phi_2=0$. Note that one of the zeros is fixed at the corner of the principal region, which is the generic behavior when N_ϕ is odd.

theta functions, are mathematically equivalent, they do differ from the computational point of view. As each theta function is computed as a sum of Gaussians with subsequently shifted arguments, it is essential that those Gaussians should be narrow. This is ensured if the parameters of those thetas have a large magnitude. Notice that τ_1 and τ_2 are pure imaginary, and

$$\lim_{\beta\to\infty}|\tau_1| = \lim_{\beta\to\infty}|\tau_2| = 2N_\phi\frac{L_2}{L_1}\sin\theta, \quad (34)$$
$$\lim_{\beta\to0}|\tau_1| = 0, \quad (35)$$
$$\lim_{\beta\to0}|\tau_2| = \infty. \quad (36)$$

Hence it is advantageous to use Eq. (18) for large β and Eq. (25) for small β. Spelling out the summations implicit in the Jacobi theta functions,

$$\rho(\mathbf{r},\mathbf{r}';\beta) = \frac{1}{\ell L_1\sqrt{\pi}}\sqrt{\frac{u}{1-u^2}}$$
$$\sum_{m=0}^{N_\phi-1}\left\{\sum_{n_1=-\infty}^{\infty}A^{(\prime)}_{0mn_1}\sum_{n_2=-\infty}^{\infty}B^{(\prime)}_{0mn_2}+\right.$$
$$\left.+(-1)^k\sum_{n_1=-\infty}^{\infty}A^{(\prime)}_{\frac{1}{2}mn_1}\sum_{n_2=-\infty}^{\infty}B^{(\prime)}_{\frac{1}{2}mn_2}\right\}, \quad (37)$$

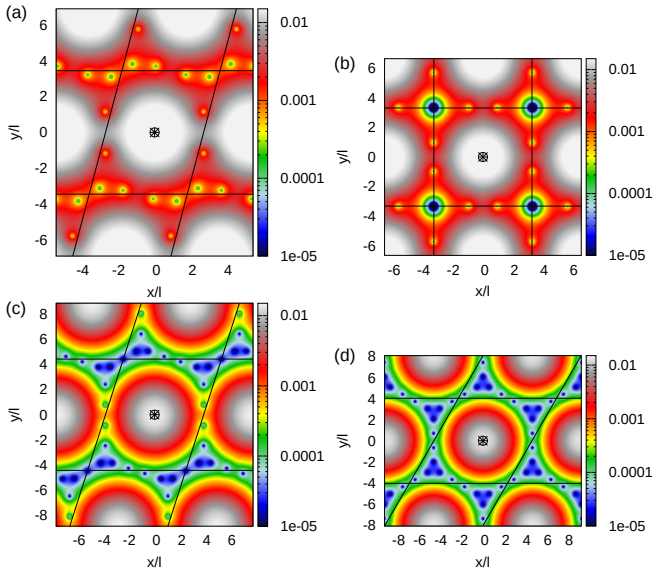

FIG. 4: The structure of zeros of the thermal density matrix for $\beta\hbar\omega_c = 200$, where the picture is stationary for different geometries and flux quanta. We show $|\rho(\mathbf{r}, \mathbf{r}'; \beta)|$, the zeros are the darkest spots. We set $\phi_1 = \phi_2 = 0$ and fix $\mathbf{r}'$ at the origin. (a) Generic torus with $N_\phi = 6$, $L_2/L_1 = 1.13$ and $\theta \approx 75°$; (b) Square principal domain ($\theta = 90°$, $L_2/L_1 = 1$) with $N_\phi = 7$; (c) Generic torus with $N_\phi = 11$, $L_2/L_1 = 1.19$ and $\theta \approx 72°$; (d) Hexagonal principal domain ($\theta = 60°$, $L_2/L_1 = 1$) with $N_\phi = 12$.

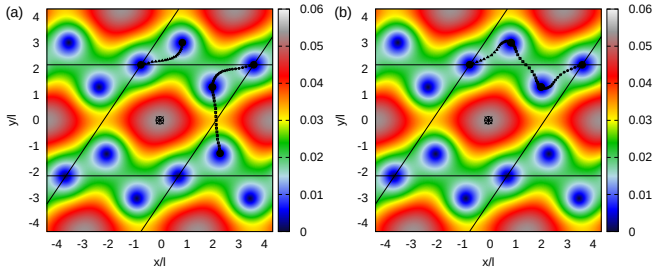

FIG. 5: The trajectory of zeros when we tune (a) the twist angle ϕ_1 and (b) the twist angle ϕ_2. We set $\beta\hbar\omega_c = 200$, $\mathbf{r}' = 0$, $N_\phi = 2$, $L_2/L_1 = 1.19$ and $\theta \approx 56°$.

where

$$A_{dmn_1} = \exp\left\{ i\pi\tau_1 \left(n_1 + a_m + d + \frac{y + y'}{2L_2 \sin\theta} \right)^2 + 2\pi i N_\phi \left(n_1 + a_m + d \right) \frac{x - x'}{L_1} \right\} \tag{38}$$

$$A'_{dmn_1} = \sqrt{\frac{i}{\tau_1}} \exp\left\{ \frac{i(x' - x)(y + y')}{2\ell^2} + \frac{\pi}{i\tau_1} \left(n_1 + N_\phi \frac{x' - x}{L_1} \right)^2 + 2\pi i n_1 \left(\frac{y + y'}{2L_2 \sin\theta} + a_m + d \right) \right\}, \tag{39}$$

and

$$B_{dmn_2} = \exp\left\{ i\pi\tau_2 \left(n_2 + d + \frac{y - y'}{2L_2 \sin\theta} \right)^2 + 2\pi i \left(n_2 + d \right) \left(N_\phi \frac{x - x'}{L_1} + 2b'_m \right) \right\}, \tag{40}$$

$$B'_{dmn_2} = \sqrt{\frac{i}{\tau_2}} \exp\left\{ \frac{i(y' - y)(x + x')}{2\ell^2} + \frac{2\pi i b'_m (y' - y)}{L_2 \sin\theta} + \frac{\pi}{i\tau_2} \left(n_2 - N_\phi \frac{x + x'}{L_1} - 2b'_m \right)^2 + 2\pi i n_2 \left(\frac{y - y'}{2L_2 \sin\theta} + d \right) \right\}, \tag{41}$$

Notice that $A'_{dmn_1} \neq A_{dmn_1}$ and $B'_{dmn_1} \neq B_{dmn_1}$, the primed and unprimed expressions are interchangeable only within the summation over n_1 and n_2, respectively. We have found it convenient to use Eq. (38) in the low-temperature range $\tanh\left(\frac{\beta\hbar\omega_c}{2}\right) > \frac{L_1}{2N_\phi L_2 \sin\theta}$, and Eq. (39) otherwise (high temperature). For the other term, B_{dmn_2} in Eq. (40) is almost always preferable to B'_{dmn_2} in Eq. (41), except if N_ϕ and θ are small and β large. Using Eq. (9), B_{dmn_2} is independent of m iff $\Re\tau$ is an integer, i.e.,

$$k' = \frac{k}{N_\phi} \tag{42}$$

is an integer. Notice that this condition is stricter than Eq. (17). (Both conditions hold trivially for a rectangular

torus.) Then, using A'_{mn_1d} in Eq. (39) and B_{mn_2d} in Eq. (40), the summation over m can be performed. If, furthermore, N_ϕ is even, an extremely compact formula is obtained:

$$\rho(\mathbf{r},\mathbf{r}';\beta) = \frac{1}{2\pi\ell^2}\frac{\sqrt{u}}{1-u}\exp\left(\frac{i(x'-x)(y+y')}{2\ell^2}\right) \times \sum_{n_1=-\infty}^{\infty} \exp\left(-\frac{1+u}{1-u}\frac{1}{4\ell^2}\left(x-x'-n_1L_1\right)^2 + +i\pi n_1\left(N_\phi\frac{y+y'}{L_2\sin\theta}+\frac{\phi_1}{\pi}\right)\right) \times \sum_{n_2=-\infty}^{\infty} \exp\left(-\frac{1+u}{1-u}\frac{1}{4\ell^2}\left(y-y'+n_2L_2\sin\theta\right)^2 + +i\pi n_2\left(N_\phi\frac{x+x'}{L_1}-\frac{\phi_2-k'\phi_1}{\pi}\right)\right). \quad (43)$$

Notice that Eq. (43) amounts to obtaining the density matrix for twisted periodic boundary from the corresponding object for the infinite plain [Eq. (1)] as the sum

$$\sum_{n_1,n_2=-\infty}^{\infty} e^{-in_1\phi_1-in_2\phi_2}t_{\mathbf{r}}(n_1\mathbf{L}_1+n_2\mathbf{L}_2)\rho^{\mathrm{open}}(\mathbf{r},\mathbf{r}';\beta). \quad (44)$$

However, the two infinite summations in this formula do not decouple unless the condition in Eq. (42) holds and N_ϕ is even. Otherwise we obtain a formula of little analytical or computational use.

IV. CONCLUSION AND OUTLOOK

We have derived several equivalent closed-form expressions for the thermal density matrix of a charged particle on the torus in a perpendicular magnetic field in Eqs. (18), (25) and (A.1). We only had to impose a mild constraint, Eq. (17), which restricts our result to a class of tori defined in terms of the side lengths and an angle of the principal domain; but the remaining class still wide enough to include both regular and oblique cases.

While this object may be of mathematical interest in its own right, we emphasize that our goal is to find a suitable starting point for path-integral Monte Carlo (PIMC) simulations. In PIMC, finite temperature expectation values are evaluated by sampling the imaginary-time path integral, discretized in units of $\Delta\tau = \beta/M$, where M is an integer. The Euclidean action, related to the logarithm of the thermal density matrix of the interacting system, can be approximated by several schemes [1] exploiting the fact that the imaginary time step, $\Delta\tau$, corresponds to a system at much higher temperature than the simulated physical system. A kinetic contribution to the action, related to the logarithm of the thermal density matrix of the *free* system, can usually be separated, and modeled as springs between particle positions on neighboring time slices. While very productive for bosonic systems, PIMC for fermions requires the fixing of the nodes of the many-body density matrix to avoid the notorious sign problem [12]. In the absence of time-reversal symmetry, which may be due either to a magnetic field for charged particles or to the Coriolis-force if motion is described in a rotating frame, however, it is necessary to fix the *phase* of the many-body density matrix. Both with node-fixing and phase-fixing, the absolute value of the density matrix is interpreted as a probability and is used in Metropolis Monte Carlo sampling.

The use of PIMC with phase fixing is often mentioned in the literature, but its practical applications are rare. This is in contrast to zero-temperature methods, where diffusion Monte Carlo with phase fixing has been applied for the study of fractional quantum Hall systems [13–15]. Apart from the issues related to phase fixing, which is more challenging at finite temperature, this is partly because PIMC simulations are usually limited to small systems, and with the density fixed, it is unavoidable that boundary conditions should play a role, especially as PIMC requires multislice sampling for efficiency, which in turn requires us to describe the free propagation for multiples of $\Delta\tau$. Our result lets us define the kinetic action in a way that is compatible with the periodicity of the torus.

Acknowledgments

This work was supported by the Hungarian Scientific Research Funds No. K105149. We thank Péter Lévay for for useful discussions. C. T. was supported by the Hungarian Academy of Sciences.

Appendix: Alternative form of the density matrix

For completeness, we note that a modular transformation $\tau_2 \to -\frac{1}{\tau_2}$, $z_2 \to \frac{z_2}{\tau_2}$ in the corresponding theta factors in Eq. (18) yields a formula that is dual to Eq. (25):

$$\rho(\mathbf{r},\mathbf{r}';\beta)=\frac{\sqrt{u}}{1+u}\frac{1}{2\ell^2 N_\phi\pi}\exp\left(-\frac{1}{4\ell^2}\frac{1-u}{1+u}|\mathbf{r}+\mathbf{r}'|^2+\frac{i(x'+x)(y'-y)}{2\ell^2}\right)$$
$$\times\sum_{m=0}^{N_\phi-1}\left(\vartheta\begin{bmatrix}a_m\\0\end{bmatrix}(z_1|\tau_1)\,\vartheta\begin{bmatrix}-2b'_m\\0\end{bmatrix}\left(\frac{z_2}{\tau_2}\middle|\tau'_1\right)+(-1)^k\vartheta\begin{bmatrix}a_m+\frac{1}{2}\\0\end{bmatrix}(z_1|\tau_1)\,\vartheta\begin{bmatrix}-2b'_m\\\frac{1}{2}\end{bmatrix}\left(\frac{z_2}{\tau_2}\middle|\tau'_1\right)\right),\quad\text{(A.1)}$$

where where $\tau'_1=\left(\frac{L_1}{2\ell N_\phi\sqrt{\pi}}\right)^4\tau_1$, and $\frac{z_2}{\tau_2}=\frac{L_1}{4\ell^2 N_\phi}\left(y-y'-i(x+x')\frac{1-u}{1+u}\right)$. Now, a change of the relative coordinates $\mathbf{r}-\mathbf{r}'$ can be turned into fluxes in the lower characteristics, and the remaining part of the arguments of the theta functions account for the periodicity of the "center-of-mass" motion.

[1] D. M. Ceperley, Rev. Mod. Phys. **67**, 279 (1995), URL http://link.aps.org/doi/10.1103/RevModPhys.67.279.

[2] A. Sarsa, K. E. Schmidt, and W. R. Magro, The Journal of Chemical Physics **113**, 1366 (2000), URL http://scitation.aip.org/content/aip/journal/jcp/113/4/10.1063/1.481926.

[3] C. Lin, F. H. Zong, and D. M. Ceperley, Phys. Rev. E **64**, 016702 (2001), URL http://link.aps.org/doi/10.1103/PhysRevE.64.016702.

[4] F. D. M. Haldane and E. H. Rezayi, Phys. Rev. B **31**, 2529 (1985), URL http://link.aps.org/doi/10.1103/PhysRevB.31.2529.

[5] F. D. M. Haldane, Phys. Rev. Lett. **51**, 605 (1983), URL http://link.aps.org/doi/10.1103/PhysRevLett.51.605.

[6] J. Zak, Phys. Rev. **134**, A1602 (1964), URL http://link.aps.org/doi/10.1103/PhysRev.134.A1602.

[7] D. Mumford, *Tata Lectures on Theta I*, Modern Birkhäuser Classics (Springer, 1987), ISBN 9780817645779, URL http://www.springer.com/us/book/9780817645724.

[8] P. Lévay, Journal of Mathematical Physics **36**, 2792 (1995), URL http://scitation.aip.org/content/aip/journal/jmp/36/6/10.1063/1.531066.

[9] N. Read and E. Rezayi, Phys. Rev. B **54**, 16864 (1996), URL http://link.aps.org/doi/10.1103/PhysRevB.54.16864.

[10] Y. Aharonov and D. Bohm, Phys. Rev. **115**, 485 (1959), URL http://link.aps.org/doi/10.1103/PhysRev.115.485.

[11] N. Byers and C. N. Yang, Phys. Rev. Lett. **7**, 46 (1961), URL http://link.aps.org/doi/10.1103/PhysRevLett.7.46.

[12] D. M. Ceperley, *Proceedings of the Les Houches Summer School, Session 56, Strongly Interacting Fermions and High Tc Superconductivity* (Elsevier, 1995), chap. 9, pp. 427–453.

[13] G. Ortiz, D. M. Ceperley, and R. M. Martin, Phys. Rev. Lett. **71**, 2777 (1993), URL http://link.aps.org/doi/10.1103/PhysRevLett.71.2777.

[14] V. Melik-Alaverdian and N. E. Bonesteel, Phys. Rev. B **52**, R17032 (1995), URL http://link.aps.org/doi/10.1103/PhysRevB.52.R17032.

[15] V. Melik-Alaverdian, N. E. Bonesteel, and G. Ortiz, Phys. Rev. Lett. **79**, 5286 (1997), URL http://link.aps.org/doi/10.1103/PhysRevLett.79.5286.